Highly Selective Indole Oxidation Catalyzed by a Mn-Containing Artificial Mini-Enzyme

Linda Leone, Daniele D'Alonzo, Ornella Maglio, Vincenzo Pavone, Flavia Nastri,* and Angela Lombardi*

ACCESS | Metrics & More | Article Recommendations | Supporting Information

ABSTRACT: Indole oxidation represents a real challenge for selectivity because it typically leads to complex mixtures of products even when highly selective enzymes are used. Here, we describe the catalytic potential of an artificial enzyme, Mn-Mimochrome VI*a (Mn-MC6*a), in promoting indole oxidation. This mini-enzyme contains a manganese—deuteroporphyrin active site within a scaffold of two synthetic small peptides covalently linked to porphyrin. Mn-MC6*a promotes the selective oxidation of indole at its C3 position, leading to a 3-oxindole derivative (2-TFE-3-oxindole) with unprecedented product selectivity (86% at pH 8.5) compared to native or artificial heme-enzymes. We also suggest a possible reaction mechanism based on the effect of pH, cosolvent, and indole substitution on the reaction outcome. These studies demonstrate that Mn-MC6*a is an excellent artificial peroxygenase for the production of 3-oxindole-containing compounds as key building blocks for the synthesis of fine chemicals.

Artificial mini-enzyme catalyzes indole oxidation with unprecedented selectivity, accessing a C2-protected 3-oxindole

KEYWORDS: metalloporphyrins, artificial metalloenzymes, indole, oxidation reactions, peroxygenase catalyst
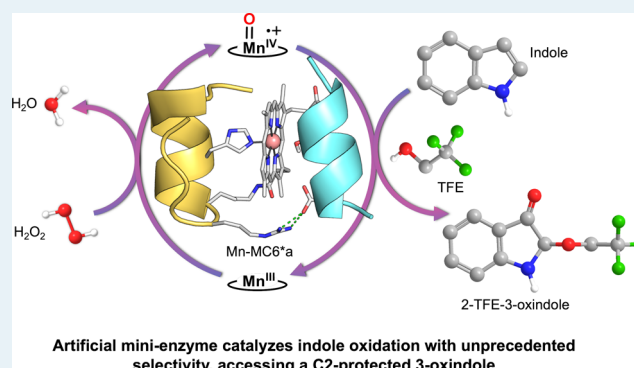
INTRODUCTION

Transition-metal catalysis is a well-established and essential tool in modern chemistry.[1] By exploiting the reactivity of a limited number of metal ions, countless transformations have been catalyzed by metal complexes, with applications ranging from medicinal[2,3] to environmental chemistry[4] and from energy production[5,6] to nanotechnology.[7] One of the major research goals in this area is the achievement of highly selective transformations, which is usually pursued by modulating the reactivity of the metal ion through first and second coordination sphere interactions.[8,9] In this context, metalloenzymes are a huge source of highly selective and naturally occurring catalysts since a complex protein environment exerts a highly specific control on the reactivity of the metal center.[10] Exploiting their evolution-driven efficiency and diversity, scientists have transferred these biocatalysts from living organisms to the work bench, applying their explosive catalytic potential to promote a plethora of synthetically useful reactions.[11−15] Among them, the selective oxygenation of organic substrates is extremely significant; hence, peroxygenases are particularly attractive enzymes for synthetic purposes.[16] Their ability to employ hydrogen peroxide as the oxygen source is advantageous for large-scale and industrial applications because of its mildness, solubility in water, and production of water as the only byproduct. Despite their unparalleled catalytic efficiency and selectivity, natural metalloenzymes typically exhibit a narrow substrate scope compared to small-molecule transition-metal catalysts as well as a more pronounced susceptibility to operating reaction conditions. Aiming to expand the catalytic repertoire of native enzymes while improving their robustness, efforts have been devoted to the construction of artificial metalloenzymes, conceived to fulfill the demand for both selectivity and versatility. Several strategies have been applied to obtain improved peroxygenases, including rational design, directed evolution, and the exploitation of decoy molecules.[16]

In this context, we have tackled the challenge through the development of miniaturized metalloporphyrin-containing proteins, named "Mimochromes" (MCs).[17] MCs can be considered as hybrid systems between metalloenzymes and small-molecule catalysts as they possess a minimal but well-designed, peptide scaffold consisting of two alpha-helical peptides, which have a covalently bound deuteroporphyrin.[18] Their functional properties have been optimized through several stages of rational design, first by constructing a
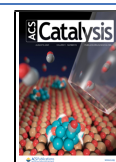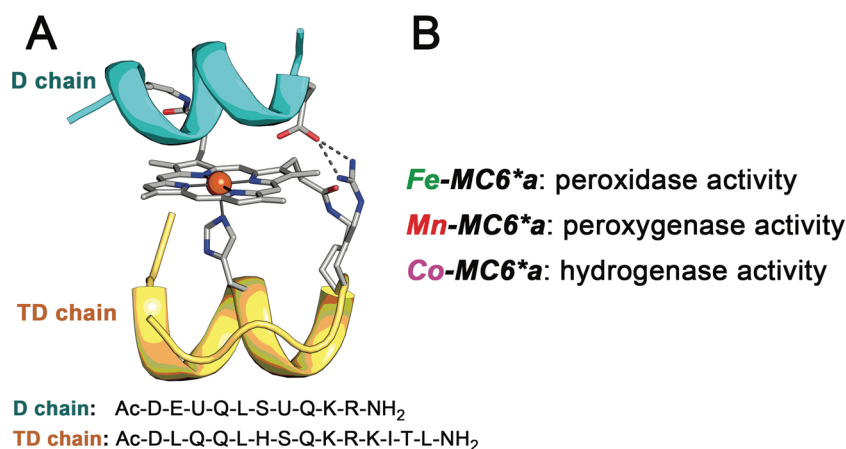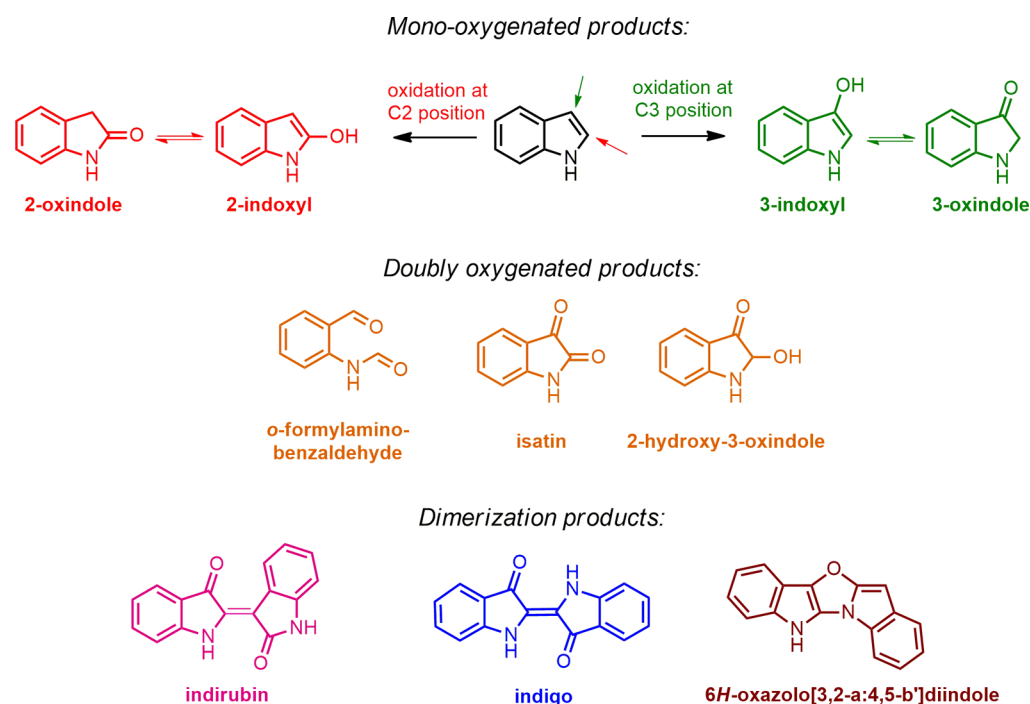
Figure 1. (A) MC6*a designed model and amino-acid sequences of its peptide chains; single letter code U stands for α-aminoisobutyric acid (Aib) residues. (B) Prevalent enzymatic activities exhibited by MC6*a in its different metal complexes.

Scheme 1. Most Representative Indole Oxidation Products

pentacoordinated, peroxidase-like, active site[19] and then by introducing punctual modifications in the peptide sequence to enhance catalyst efficiency[20] and robustness.[21] Among the MCs, we have identified Mimochrome VI*a (MC6*a, Figure 1A) as the most promising candidate for catalysis, and we have screened its iron, manganese, and cobalt complexes for diverse reactivities (Figure 1B).[21−23]

Particularly important is the ability of Mn-MC6*a to promote the chemoselective oxygenation of thioethers upon activation of hydrogen peroxide, acting through a direct oxygen transfer pathway rather than a one-electron stepwise mechanism.[22] The encouraging results outlined in our previous work prompted us to widen the scope of transformations catalyzed by Mn-MC6*a in oxidation chemistry. Therefore, we selected indole oxidation as an intriguing reaction to evaluate the ability of Mn-MC6*a in promoting selective substrate oxygenation. Despite the structural simplicity of the indole molecule, its oxidation generally leads to a large number of

products, including mono-oxygenated, doubly oxygenated, and dimeric compounds (Scheme 1).

The oxygenated derivatives of indole have gathered significant interest in different areas of research and industry. Among them, indigo is one of the oldest dyes that has been employed in textile coloration owing to its highly intense blue color. The stable pink isomer of indigo, known as indirubin, has also been largely used as a dye, and its derivatives have recently displayed diverse pharmacological activities.[24] Mono-oxygenated 2- or 3-oxindoles are valuable scaffolds for drug design[25] and their derivatives have found application in the treatment of several diseases, including cancer,[26] diabetes,[27] and also protozoan[28] and viral infections.[29] Although 2-oxindole is a stable and commercially available molecule, accessing 3-oxindole is quite difficult due to the high susceptibility of this compound to spontaneous oxidation.[30] Several approaches have been developed to obtain the 3-oxindole scaffold through organic synthesis or by transition-
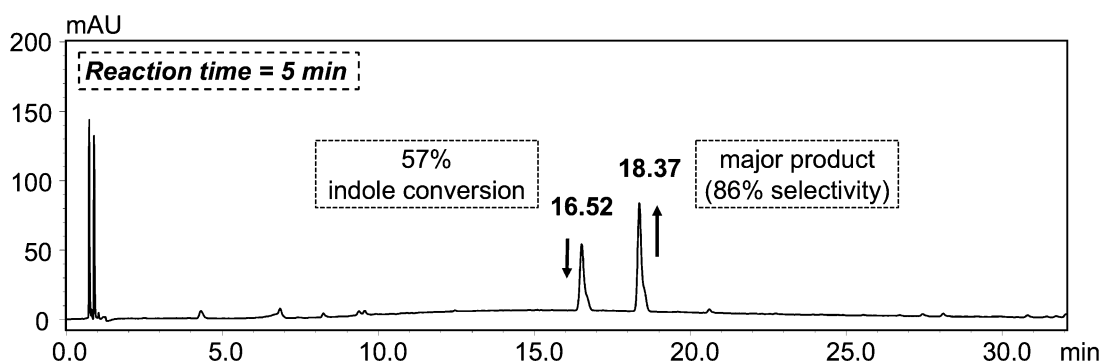
Figure 2. RP-HPLC profile at λ = 240 nm of indole oxidation catalyzed by Mn-MC6*a in 60 mM sodium phosphate at pH 8.5 in the presence of 40% v/v TFE. Analysis was performed after 5 min after H_2O_2 addition. Peaks at 16.52 and 18.37 min represent indole and its major oxidation product, respectively. Arrows indicate changes in peak intensities during reaction.

Scheme 2. Proposed Reaction Mechanism for Indole Oxidation Catalyzed by Mn-MC6*a at pH 8.5[a]
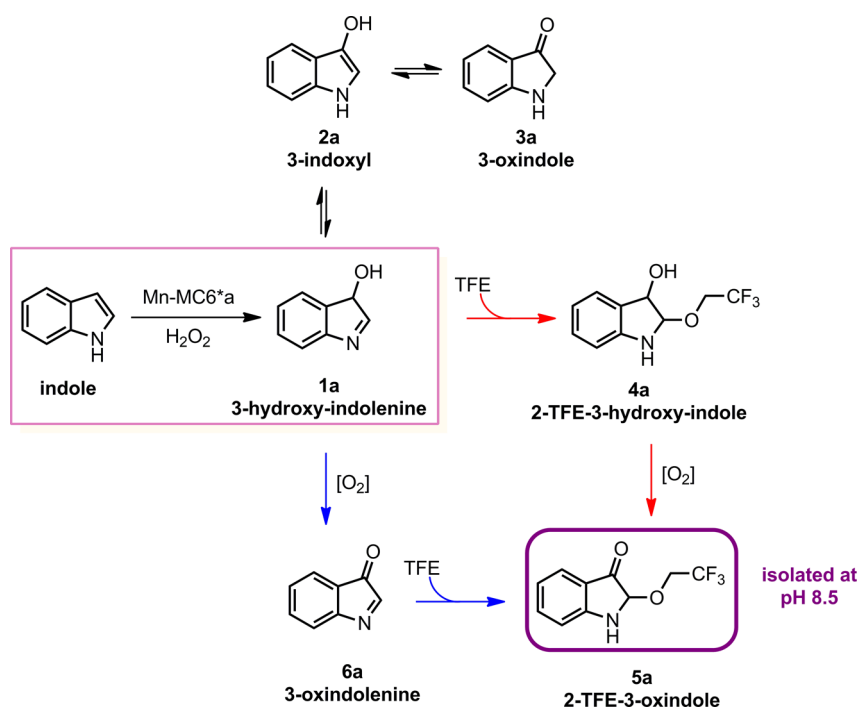
[a]The selective C3 hydroxylation of indole promoted by Mn-MC6*a is highlighted in the pink box. Red arrows indicate one possible pathway for the formation of the observed product (2-TFE-3-oxindole, purple contour), while blue arrows indicate the same reaction steps occurring in the reverse order.

metal catalysis. They usually involve post-oxidation indole assembly strategies rather than the direct oxygenation of indole[31−34] as the latter typically provides multiple products. Among metalloenzymes, several heme-proteins have been screened as catalysts for indole oxidation, including myoglobin (Mb),[35] chloroperoxidase (CPO),[36,37] cytochromes P450 (P450s),[38] dehaloperoxidase (DHP),[39] and indoleamine 2,3-dioxygenase (IDO).[40] Each enzyme catalyzes the reaction with different product distributions, but no significant selectivity toward any of the oxidation products has been observed in most cases. As a unique exception, CPO displayed marked selectivity toward the formation of 2-oxindole.[36] In contrast to native proteins, the recently reported Mb mutant (F43Y Mb) promotes the selective formation of indigo (80% selectivity) from indole.[41] Small-molecule catalysts, such as synthetic metalloporphyrins, have also been screened for indole oxidation.[42−44] A comparative study between Fe- and Mn-based metalloporphyrins evidenced different product selectivities, depending on the nature of the metal ion, with the Mn-containing catalyst displaying moderate selectivity (64%) toward 2-oxindole and the Fe-analogue producing modest amounts of indigo (20% selectivity).[42] Even though mechanistic hypotheses have been proposed to explain the product distribution observed in each case, the detailed mechanism of heme-catalyzed indole oxidation still remains not completely understood.[39−41]

Here, we report indole oxidation catalyzed by Mn-MC6*a and show that this catalyst is able to regioselectively convert the substrate, promoting indole oxidation at the C3 position. Interestingly, the presence of 2,2,2-trifluoroethanol (TFE) as a cosolvent, required for driving MC helical folding and enhancing the catalytic performances, allowed us to shed light on the observed selectivity. TFE actively participates in the stabilization of a highly reactive indole oxidation product.

We were able to isolate and fully characterize 2-(2',2',2'-trifluoroethoxy)-3-oxindole (2-TFE-3-oxindole) as a solvent-trapped indole oxidation derivative. Furthermore, we propose a possible reaction mechanism by evaluating the effect of indole substitutions and of different alcohols on the reaction outcome.

RESULTS

Indole Oxidation by Mn-MC6*a. Indole oxidation catalyzed by Mn-MC6*a was performed in the presence of an equimolar amount of hydrogen peroxide as the terminal oxidant (10 μM Mn-MC6*a, 1 mM H_2O_2, and 1 mM indole). The reaction was performed in an aqueous solution containing TFE (40% v/v) as a cosolvent, which has widely been shown to increase the MC catalytic performance by stabilizing the overall folding.[21,22]

Mn-MC6*a acted as a fast and selective catalyst for indole oxidation, promoting 57% conversion of indole into the main oxidation product (86% selectivity) within 5 min at pH 8.5 (Figure 2). No reaction progress was observed for the uncatalyzed oxidation over the same timescales, thus proving the involvement of Mn-MC6*a in driving indole oxidation. Control experiments were also performed in the presence of Mn-deuteroporphyrin IX (Mn-DPIX) as the catalyst under the best reaction conditions observed for Mn-MC6*a (pH 8.5, 40% TFE v/v). Experiments were carried out in the absence and in the presence of 1 eq imidazole as a cocatalyst, and they revealed no substrate consumption over at least 60 min. This finding further corroborates that the interactions between metalloporphyrin and the peptide chains drive the metal-cofactor reactivity.

Liquid chromatography—electrospray ionization (LC-ESI) high-resolution mass spectrum and UV—vis absorption profile of the main reaction product (Figure S1) were consistent with those reported in the literature for 3-oxindolenine (6a, Scheme 2), which was already observed, as a minor product, in indole oxidation catalyzed by DHP.[39] However, comparison of its retention time in reverse-phase high-performance liquid chromatography (RP-HPLC) analysis with literature data suggested higher lipophilicity of the product formed in Mn-MC6*a-catalyzed indole oxidation with respect to the previously reported 3-oxindolenine.[39]

In order to unequivocally identify the product, the reaction was scaled up and the mixture was purified by preparative RP-HPLC. Nuclear magnetic resonance (NMR) characterization of the pure product (Figures S2—S5) allowed us to identify it as 2-TFE-3-oxindole (5a, Scheme 2). This derivative presumably results from nucleophilic addition of TFE to 3-oxindolenine. In the high-resolution mass spectrum, the product displayed an *m/z* value consistent with the exact mass of 3-oxindolenine, presumably due to the acid-catalyzed elimination of TFE in the ESI source. Indeed, gas chromatography electron impact-mass spectrometry (GC-EI-MS) analysis under nonacidic conditions revealed an experimental mass of 231.1 Da (Figure S6), consistent with the 2-TFE-3-oxindole molecular structure, as assigned by NMR analysis. The difference (100.0 Da) observed between LC-ESI-MS and GC-EI-MS experimental masses exactly corresponds to the mass of TFE.

Properties of the TFE-Trapped Indole Oxidation Product. The above results demonstrate that indole oxidation, catalyzed by Mn-MC6*a, led to a product in which a cosolvent TFE molecule is incorporated at the C2 position of 3-oxindole. This compound is a highly interesting intermediate from a synthetic point of view as it is well suited for the construction of various synthetic targets[45] through substitution of the trifluoroethoxy group with appropriate nucleophiles.[46,47] 2-TFE-3-oxindole is characterized by a high electrophilic character at the C2 position, similarly to 3-oxindolenine. As a proof of such reactivity, 2-TFE-3-oxindole was gradually converted into multiple reaction products when the oxidation reaction was carried out for longer times (up to 60 min) at pH 8.5 (Figure S7 and Table S1). Among them, the predominant peak detected by RP-HPLC analysis was assigned to the doubly oxygenated indole-2,3-dione (isatin), based on UV—vis absorption and ESI-MS analysis (Figure S8), by comparison with the standard compound.

The purified 2-TFE-3-oxindole was stable over several days in diluted organic solution (mM concentration in acetonitrile, dimethylsulfoxide, or ethyl acetate), allowing for a complete NMR characterization (Figures S2—S5). However, it was spontaneously oxidized to indigo upon concentration by solvent evaporation under aerobic conditions. In neutral aqueous solution, 2-TFE-3-oxindole underwent nucleophilic substitution with H_2O, resulting in 2-hydroxy-3-oxindole (Figure S9A).

This species shows a lower retention time in the RP-HPLC analysis and a comparable UV—vis absorption profile with respect to 2-TFE-3-oxindole (Figure S9B,C). 2-Hydroxy-3-oxindole was identified based on ^{1}H-NMR (Figure S10) and GC-EI-MS (Figure S11) analysis (experimental mass 149.1 Da).

Effect of pH and Different Alcohols on the Reaction Outcome. The effect of pH on indole oxidation in the presence of TFE was examined in order to investigate the involvement of the Mn^{IV}-oxo species in the reaction, according to previous findings.[22] The reaction provided higher indole conversions within 5 min at higher pH values (Figure 3).
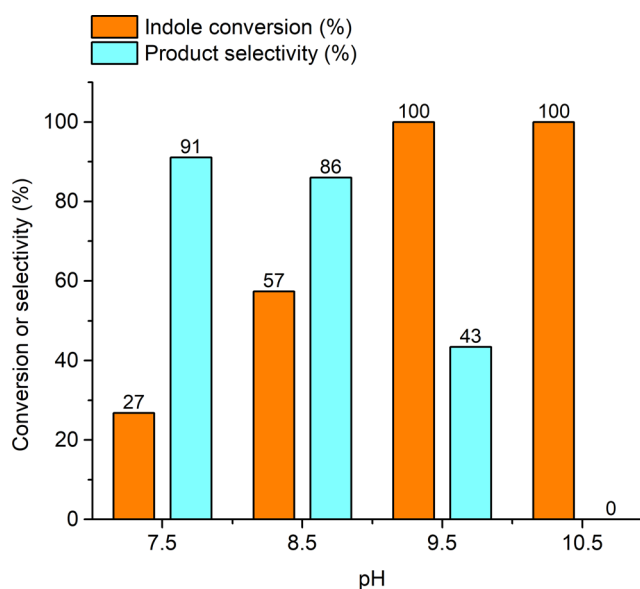
Figure 3. pH-dependent oxidation of indole catalyzed by Mn-MC6*a. Orange bars indicate the indole overall conversions observed after 5 min of reaction progress; light blue bars indicate product selectivity as percentage of 2-TFE-3-oxindole formed over all reaction products. Reaction conditions: Mn-MC6*a, 10 μM; H_2O_2, 1 mM; and indole 1 mM; different buffers were used depending on the pH value as described in the Experimental Section.

Scheme 3. Proposed Mechanism for the Formation of the Main Products in the Mn-MC6*a-Catalyzed Indole Oxidation at Different pH Values[a]
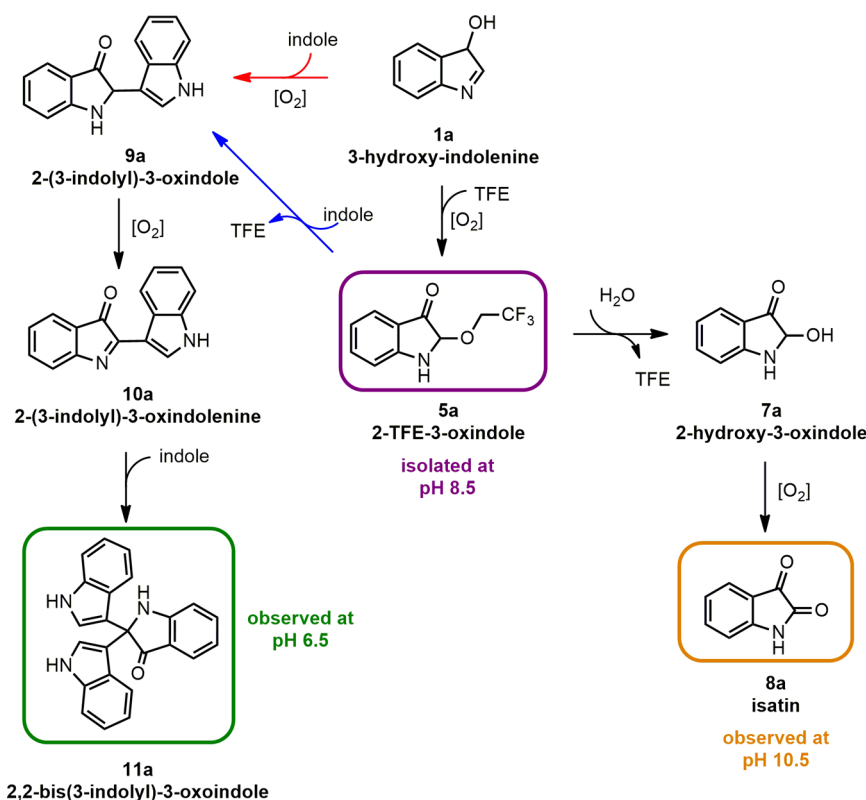
[a] All the observed products are conceived to be formed from **1a**, which results from indole C3 oxygenation by Mn-MC6*a. Green contour: major product observed at pH = 6.5 with a long reaction time; purple contour: major product observed at pH = 7.5 and 8.5; orange contour: major product observed at pH = 10.5.

Simultaneously, selectivity toward 2-TFE-3-oxindole decreased on increasing the pH, and a complex product distribution was detected at pH 10.5 (Figure S12), with a significant amount of isatin (22%) after 5 min.
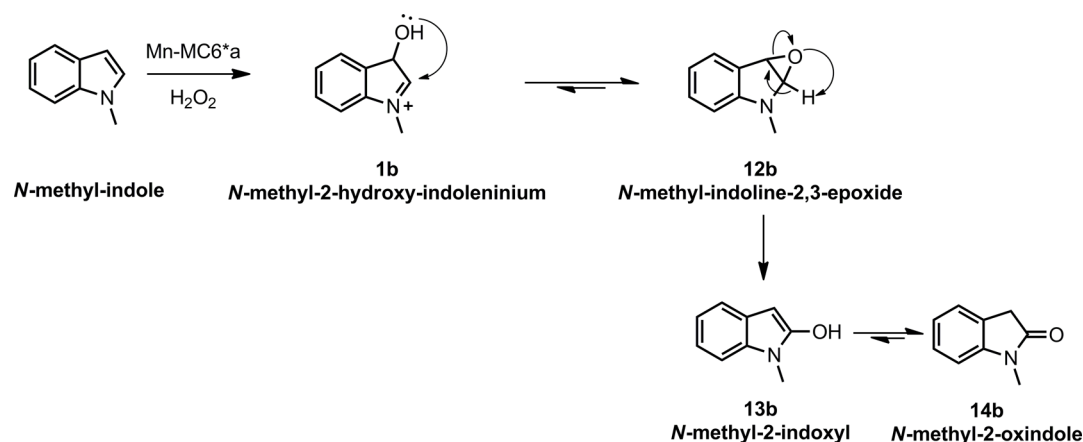
When the reaction was carried out at pH 6.5, no significant indole consumption was detected after 5 min, and longer reaction times were required for conversion (53% after 1 h). Interestingly, a different product distribution was observed (Figure S13). The predominant species, identified by LC-high-resolution mass spectrometry (HRMS) analysis, correspond to the pseudo-trimer 2,2-bis(3′-indolyl)-3-oxoindole (Figure S14A) and 2-hydroxy-3-oxindole (Figure S14B). The former species has been reported in the literature as a product of biocatalytic indole oxidation and was postulated to derive from 3-indoxyl.[48] Small amounts of 2-TFE-3-oxindole, and a pseudo-dimeric species (Figure S14C), possibly resulting from the coupling of 3-oxindolenine and indole, were also detected.

Under the best pH condition (8.5), in terms of yield and selectivity, the effect of different alcohols on the Mn-MC6*a-catalyzed indole oxidation was investigated. When methanol (MeOH) or ethanol (EtOH) was used as a cosolvent (40% v/v), the reaction proceeded with lower substrate conversions (31 and 44% after 5 min, respectively), and 2-methoxy- and 2-ethoxy-3-oxindole were detected as products, respectively (Figures S15−S18). Indole oxidation was also performed in an aqueous solution at pH 8.5 and in the absence of cosolvents (Figure S19), leading to 28% conversion after 5 min. In this case, 2-hydroxy-3-oxindole and isatin were formed as products.

The different conversions observed with TFE, EtOH, MeOH, and H$_2$O likely reflect the different capabilities of these solvents to stabilize MC6*a folding, as determined by circular dichroism (CD) spectroscopy (Figure S20 and Table S2). For all the screened cosolvents, the formation of solvent adducts such as 3-oxindole derivatives strongly suggests that alcohol addition occurs subsequently to indole C3 oxygenation by Mn-MC6*a. Similarly, in the absence of cosolvents, addition of H$_2$O to the primary C3 oxygenation product leads to 2-hydroxy-3-oxindole. Aerobic oxidation of the latter conceivably gives rise to isatin.

Mechanistic Implications. All the obtained results provided first indications toward a mechanistic hypothesis for the observed reaction outcome (Scheme 2). Experimental evidence indicates that Mn-MC6*a selectively promotes indole oxygenation at the C3 position. In line with the pH-dependent Mn-MC6*a Compound I formation,[22] the manganyl-oxo species was proposed as the active oxidizing intermediate, which mediates the C3 oxygenation of indole.

Regardless of whether this reaction occurs through a direct oxygen transfer or a stepwise "oxygen-rebound" mechanism,[49] it is expected to give 3-hydroxy-indolenine as the first oxidation product (**1a**, Scheme 2), which is involved in a tautomeric equilibrium with 3-indoxyl (**2a**) and 3-oxindole (**3a**) in aqueous solution. However, none of these species was detected under the explored experimental conditions and 2-TFE-3-oxindole (**5a**) was isolated as the main reaction product. The observed behavior may be explained through the nucleophilic addition of TFE to **1a** (Scheme 2, red arrows) followed by the

Scheme 4. Possible Reaction Pathway for *N*-methyl-2-oxindole Formation Promoted by Mn-MC6*a[a]

N-methyl-indole　　　　1b　　　　12b
　　　　　　　　N-methyl-2-hydroxy-indoleninium　　*N*-methyl-indoline-2,3-epoxide

13b　　　　　　14b
N-methyl-2-indoxyl　　*N*-methyl-2-oxindole

[a]The proposed mechanism first involves C3 hydroxylation of the substrate and the subsequent epoxide ring closure from **1b**.

benzylic oxidation of the resulting 2-(2′,2′,2′-trifluoroethoxy)-3-hydroxy-indole (2-TFE-3-hydroxy-indole, **4a**) in the presence of ambient O_2, leading to the observed product **5a**. The same product is expected to be formed even if these two steps would occur in a reverse order (Scheme 2, blue arrows), with the benzylic oxidation of **1a**, affording 3-oxindolenine (**6a**), followed by nucleophilic addition of TFE.

In order to probe the role of dioxygen in the formation of the observed products, indole oxidation was carried out under a nitrogen atmosphere at pH 8.5 and in the presence of TFE. RP-HPLC analysis performed after 5 min of the reaction revealed that the formation of 2-TFE-3-oxindole and isatin is inhibited in the absence of O_2 (Figure S21), according to the proposed reaction pathway.

Scheme 3 illustrates the proposed mechanism for the formation of indole oxidation products at various pH values. The formation of isatin (**8a**, Scheme 3) has been hypothesized as resulting from nucleophilic substitution of OH^-/H_2O to 2-TFE-3-oxindole, leading to 2-hydroxy-3-oxindole (**7a**, Scheme 3), followed by further spontaneous oxidation by ambient O_2 at the C2 position. The former reaction is favored under alkaline conditions, as suggested by the increased isatin production at pH 10.5. On the other hand, at pH 6.5, it is reasonable to hypothesize that the coupling reaction of indole with 3-hydroxy-indolenine (Scheme 3, red arrow) competes with TFE addition, leading to pseudo-dimeric 2-(3-indolyl)-3-oxindole (**9a**) after oxidation at the benzylic position. The latter species could also result from substitution of TFE with indole on **5a** (Scheme 3, blue arrow). Indeed, due to slower substrate consumption by Mn-MC6*a at this pH, small amounts of **5a** are formed along with an excess of unreacted substrate. Once species **9a** is formed, it is spontaneously oxidized by O_2 to give 2-(3-indolyl)-3-oxindolenine (**10a**), detected in small amounts during the reaction (Figures S13 and S14C). A final coupling reaction, involving a further indole molecule as the nucleophile, would afford the observed pseudo-trimeric compound **11a**. Since the formation of **11a** relies on the competitive addition between TFE and unreacted indole to **1a**, the effect of substrate concentration at pH 6.5 was evaluated. Product selectivity toward the pseudo-trimeric compound **11a** increased from 45% at 1 mM to 70% at 10 mM indole concentration, in agreement with the proposed mechanism.

Interpreting Selectivity: Oxidation of *N*-Substituted Indoles by Mn-MC6*a. In order to decipher the reaction pathway for indole oxidation proposed in Scheme 2, the effect of indole substitution on product distribution was examined. *N*-methyl-indole was chosen as the substrate since the amino group derivatization was expected to increase substrate reactivity at the C3 position and enhance the electrophilic character at the C2 position after insertion of the C3 hydroxyl group.

When the Mn-MC6*a-catalyzed oxidation of *N*-methyl-indole was carried out at pH 8.5, the reaction selectivity was altered, and remarkably, *N*-methyl-2-oxindole (**14b**, Scheme 4) was detected as the main product (Figure S22).

In line with the literature data,[43] formation of **14b** is the result of an internal rearrangement reaction, occurring from *N*-methyl-indoline-2,3-epoxide (**12b**, Scheme 4).

Epoxidation reactions by Mn-complexes and metalloporphyrins are widely described in the literature.[50,51] Possible pathways involve the addition of the manganyl-derived oxygen to the double bond either in a concerted manner or through one- or two-electron stepwise processes. The preferred mechanism depends on several factors including the redox potential of the active oxidant and the reactivity of the substrate and of the putative intermediate. Since *N*-methyl-indole is characterized by a higher nucleophilic character at the C3 position with respect to indole, the reaction mechanism is expected to involve C3 oxygenation also in this case (Scheme 4). At this stage, formation of *N*-methyl-3-oxindolenine from **1b** is disfavored as it would retain a positive charge. As a consequence, the electrophilic character at the C2 position of **1b** is greatly enhanced compared to **1a**; thus, it is conceivable that the C3 hydroxyl group of **1b** successfully competes with TFE in the nucleophilic attack to C2, leading to epoxide **12b**. In order to support our mechanistic hypothesis, an electron-withdrawing substituent was introduced, and *N*-acetyl-indole was screened as the substrate. In the reaction carried out at pH 8.5, no product formation was observed (Figure S23), further indicating that indole reactivity toward Mn-Compound I relies on electron donation from the nitrogen toward the C3 position.

All these data strongly suggest a common reaction mechanism for the oxidation of indole and *N*-methyl-indole, involving the selective C3 oxygenation of the substrates, mediated by the manganyl-oxo species (Scheme 5).

Scheme 5. Proposed Mechanism for Oxidation of Indoles by Mn-MC6*a
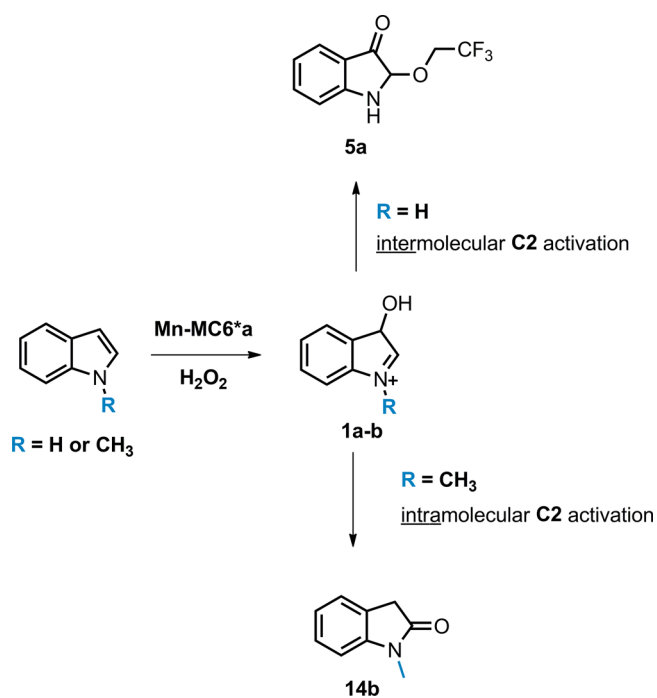
In order to investigate the mechanism of the oxygenation reaction, isotopic labeling experiments were performed with both indole and N-methyl-indole using $H_2^{18}O_2$ as the oxidant. N-methyl-2-oxindole fully incorporated ^{18}O (Figure S24), thereby suggesting an oxygen transfer mechanism mediated by Mn-Compound I, rather than a radical pathway. Conversely, a very low percentage of ^{18}O incorporation into 2-TFE-3-oxindole was observed (data not shown). This finding is not completely unexpected considering that the carbonyl group of this product could undergo oxygen exchange with the solvent,[52] as a consequence of an acetalization equilibrium.

In order to test this hypothesis, label exchange experiments were performed by treating isolated 2-TFE-3-oxindole with labeled water ($H_2^{18}O$) at pH 8.5 with 40% v/v TFE. The product gradually incorporated labeled oxygen (Figure S25), thus indicating that its carbonyl group actually undergoes oxygen exchange with the solvent. The same experiment performed with N-methyl-2-oxindole did not show any ^{18}O incorporation, confirming the stability of this product to solvent exchange.

All these results suggest that a direct oxygen transfer from the Mn^{IV}-oxo species to both substrates occurs. It should also be noticed that the product distribution of indole oxidation was not affected by the presence of D-mannitol as a hydroxyl radical scavenger[39,40] (Figure S26), further pointing out to a direct oxygen transfer rather than a stepwise, oxygen-rebound mechanism.

■ DISCUSSION

Regioselectivity in indole oxidation mostly relies on the mechanism of oxygen addition to the C2−C3 double bond of the substrate. Formation of 2-oxindole likely results from an epoxidation pathway, while the route to 3-oxindole and related products (3-oxindolenine, 2-hydroxy-3-oxindole, and indigo) derives from C3 hydroxylation.[43] The first mechanism appears predominant in heme-thiolate enzymes as 2-oxindole is observed as the only product in the presence of CPO[36,37] and is predominant with P450s.[38] The latter enzymes also produce significant amounts of 6H-oxazolo[3,2-a:4,5-b′]-diindole, which results from the coupling of indole with the 3-indoxyl radical. This last finding suggests an intricate reaction pathway for the P450-catalyzed reaction, involving one- and two-electron oxidation steps. Conversely, a C3 hydroxylation pathway has been observed with the artificial enzyme F43Y Mb, which promotes the formation of indigo from indole, resulting from formation and coupling of 3-indoxyl radicals.[35,41] An intermediate reactivity has been reported for IDO and DHP, which yield mixtures of both 2- and 3-oxygenated products in different amounts.[39,40]

Unlike all the aforementioned examples, Mn-MC6*a oxidizes indole with an unprecedented selectivity. This catalyst preferentially promotes indole oxygenation at the C3 position, yielding a 3-oxindole derivative as the main product. Despite the similarities with F43Y Mb in the regioselectivity,[41] the reaction outcomes achieved by Mn-MC6*a catalysis are peculiar. Unlike natural proteins, this mini-enzyme requires the presence of TFE as the cosolvent to enhance its folding, and consequently, its reactivity. In peroxidase-like reactions, TFE has the only effect of boosting catalyst stability and reactivity,[20,21] while in the case of indole oxidation, the cosolvent works in synergy with the catalyst allowing for the isolation of a highly reactive compound. Formation and isolation of 2-TFE-3-oxindole highlight the ability of Mn-MC6*a to promote indole oxidation selectively at its C3 position. Moreover, it also indicates the crucial role of TFE in minimizing subsequent side reactions of the product. Indeed, it is well known that 3-oxindole is spontaneously oxidized to indigo in an alkaline solution and in the presence of oxygen, possibly involving 3-oxindolenine as an intermediate.[30]

The use of different alcohols as cosolvents affords analogous 2-alkoxy-3-oxindole derivatives with lower yields, underlying the effectiveness of the Mn-MC6*a−TFE system in providing a C2-functionalized 3-oxindole. The selectivity of Mn-MC6*a toward the C3 position of indole is evidenced by the negligible amounts of 2-oxindole detected under all the explored reaction conditions. The lack of indigo formation during the Mn-MC6*a-catalyzed reaction also suggests the absence of radical pathways, indicating a preferred 2-electron over 1-electron oxidation by Mn-MC6*a. Notably, Mn-MC6*a-catalyzed indole oxidation is altered upon substrate modification. The cases herein examined revealed the ability of the catalyst to afford different oxidation products, depending on indole nitrogen substitution. To explain this behavior, a common reaction mechanism has been proposed for both the screened indoles with Mn-MC6*a promoting a 2-electron oxidation coupled to C3 oxygenation. In this scenario, the formation of N-methyl-2-oxindole also results from C3 oxygenation of N-methyl-indole, but the fate of the primary oxidation product (1a-b, Scheme 5) is then driven by the reactivity of the adjacent C2 center. Isotopic labeling studies using $H_2^{18}O_2$ finally provided an indication of peroxygenase activity, reinforcing the hypothesis of a direct oxygen transfer mechanism. However, alternative pathways cannot be ruled out, mainly for indole, and further mechanistic studies would be required to completely decipher the reaction mechanism.

The peculiar reactivity of Mn-MC6*a compared to both small-molecule metalloporphyrins and heme-proteins suggests that peptide−porphyrin interactions could have a role in determining the reaction selectivity. Experiments performed

with the isolated Mn-DPIX complex, under the same conditions used for Mn-MC6*a, highlight that the peptide scaffold is essential for disclosing the reactivity of the Mn center. However, due to the minimal dimensions of the Mn-MC6*a scaffold, the active site is quite wide and solvent-accessible. Therefore, it is difficult to predict specific interactions that would drive the reaction selectivity. It is conceivable that the peptide scaffold modulates the electronic properties of the Mn center, favoring a C3 hydroxylation mechanism over other possible pathways. Theoretical studies concerning the energetic aspects of Mn-MC6*a-mediated indole oxygenation are currently under way and will be reported in the following study.

CONCLUSIONS

This work demonstrates the exceptional potential of Mn-MC6*a as a catalyst for key synthetic transformations. In summary, this artificial mini-enzyme selectively promotes the oxidation of indole at its C3 position, leading exclusively to the formation of a 3-oxindole derivative (2-TFE-3-oxindole) in which a solvent molecule (TFE) is incorporated at the C2 position of the oxidized product. The presence of TFE in the indole oxidation reaction promoted by Mn-MC6*a has a twofold favorable effect. TFE not only strengthens catalysis by stabilizing the catalyst folding but also it behaves like a reagent and provides an oxidized indole derivative, functionalized at the most reactive C2 position. The 2-TFE-3-oxindole product may represent a new and unique starting material for subsequent synthetic transformations.

Mn-MC6*a is one of the most proficient catalysts for indole oxidation as it provides complementary selectivity by varying substrate substitution. The remarkable reactivity of Mn-MC6*a compared to small-molecule metalloporphyrins and heme-proteins also indicates that the peptide scaffold plays a crucial role in directing reaction selectivity. Although native protein architectures do not succeed in steering indole oxidation toward a single reaction product, our minimal system achieves the highest selectivity reported so far in metalloporphyrin-catalyzed indole oxidation. Future developments will focus on dissecting reasons for such selectivity while expanding the range of transformations accessible to these simple but highly versatile mini-enzymes.

EXPERIMENTAL SECTION

Mn-MC6*a was synthesized as previously described by us.[22] Stock solutions of Mn-MC6*a were prepared by dissolving the pure, lyophilized compound in H_2O 0.1% TFA (v/v) at ~0.5 mM. Concentrations were determined spectrophotometrically using the molar extinction coefficient (ε_{365}) of 7.9×10^4 M^{-1} cm^{-1}.[22] Stock solutions of H_2O_2 were prepared by proper dilution of a commercial stock solution (30% w/w in H_2O) and their concentration was determined using $\varepsilon_{240} = 39.4$ M^{-1} cm^{-1}.[53] Stock solutions of indoles were freshly prepared by dissolving a weighted amount of the pure compound in TFE. Mn-DPIX was synthesized following a slightly modified literature procedure.[54] DPIX dihydrochloride (100 mg) was dissolved in dimethylformamide (DMF) to 15 mM concentration, and the mixture was heated to reflux. Then, Mn(II) acetate (10 eq) was added, and the reaction was followed by thin-layer chromatography (TLC) (CH_2Cl_2:MeOH 7:3). Mn-insertion into DPIX was completed after 2 h, as also ascertained by monitoring the UV−vis spectrum, which was

in agreement with the literature data.[55] The reaction mixture was cooled to room temperature and the crude product was dried under vacuum. Purification of Mn-DPIX from excess of Mn(II) acetate was performed by reverse-phase flash chromatography with a Biotage Isolera system. A SNAP KP C18 60 g cartridge was used for the purification, eluted with a linear gradient of acetonitrile in H_2O containing 0.1% TFA. The fractions containing the pure product were concentrated under vacuum and lyophilized. Stock solutions of Mn-DPIX were prepared by dissolving a known amount of the product in DMF. All solutions were stored at −20 °C until their use.

In the $H_2{}^{18}O_2$ labeling studies, a solution of 90% ^{18}O-enriched hydrogen peroxide at 3% (w/w) concentration in $H_2{}^{16}O$ was used. In the $H_2{}^{18}O$ solvent exchange experiments, 100 mM phosphate buffer of pH 8.5 was prepared using 99% ^{18}O-enriched H_2O and appropriately diluted with TFE and stock solutions of 2-TFE-3-oxindole or N-methyl-2-oxindole. In particular, 5 μL of the product stock solution (10 mM in TFE) and 195 μL of TFE were added to 300 μL of $H_2{}^{18}O$-labeled phosphate buffer, affording ~60% final ^{18}O concentration in the total reaction volume.

Reactions were started by addition of H_2O_2 (1 mM) to a stirring mixture of the catalyst (10 μM) preloaded with the substrate (1 mM) in an appropriate buffer (60 mM) containing 40% TFE (v/v). Sodium phosphate was used in the reactions at pH 6.5, 7.5, and 8.5, while sodium carbonate was used at pH 9.5 and 10.5. Aliquots of the reaction mixture (50 μL) were taken at given times (from 5 to 120 min), diluted with H_2O (50 μL), and analyzed by RP-HPLC. RP-HPLC analyses were performed with a Kinetex Phenyl-Hexyl column (150 mm × 4.6 mm, 5 μm) using water with 0.1% TFA (A) and acetonitrile with 0.1% TFA (B) as the eluents. A linear gradient from 5 to 50% B over 30 min at a flow rate of 1.85 mL/min was used as the elution method in all analyses.

The degree of indole conversion and the yield of 2-TFE-3-oxindole were calculated by RP-HPLC peak integration based on external calibration using standard solutions (Figure S27). Product selectivity was also determined by integration of nonoverlapping peaks in the ^{1}H-NMR spectrum of the crude reaction mixture. For the NMR analysis, the reaction mixture (2 mL) was extracted with ethyl acetate (4 mL) to remove the catalyst. The organic phase was dried under nitrogen and then resuspended in acetonitrile d_3 (0.7 mL). RP-HPLC analysis of the sample confirmed that product distribution was not altered during the procedure (Figure S28). NMR spectra of authentic indole, isatin, and 2-TFE-3-oxindole in acetonitrile d_3 were also collected. Formation of 2-hydroxy-3-oxindole was followed by monitoring the NMR spectrum of 2-TFE-3-oxindole dissolved in D_2O over time (Figure S10).

Isolation and purification of 2-TFE-3-oxindole were performed by extraction of the reaction mixture (50 mL) at pH 8.5 after 15 min using ethyl acetate (100 mL). The organic phase was dried with sodium sulfate, concentrated under vacuum, and then completely evaporated under nitrogen. The crude reaction mixture was redissolved in pure H_2O (8 mL). The sample was purified by preparative RP-HPLC with a Vydac C18 column (250 mm × 10 mm, 5 μm) using water (A) and acetonitrile (B) as the eluents. A linear gradient from 5 to 50% B for over 50 min at a flow rate of 4.5 mL/min was used as the elution method. The fraction containing the pure product was extracted with ethyl acetate straight after the purification. The product purity and its identity were confirmed by GC−MS analysis.

GC analysis was performed using an Rxi-5Sil MS column with helium as the carrier gas. A linear gradient from 80 to 230 °C with a rate of 18 °C min^{-1} was used. MS analysis was performed in the total ion current (TIC) mode, exploring a range of m/z values from 50 to 300 Th. Crystals of pure 2-TFE-3-oxindole were obtained by careful evaporation of the solvent (hexane:ethyl acetate 9:1) at 4 °C.

^{1}H NMR, ^{13}C NMR, and ^{19}F NMR spectra were recorded using Bruker Avance 600 or 400 MHz spectrometers. All the NMR experiments were carried out at 298 K. 2D spectra (double-quantum filtered correlation spectroscopy (DQF-COSY), ^{1}H−^{13}C heteronuclear single-quantum coherence (HSQC) spectroscopy, and ^{1}H−^{13}C heteronuclear multiple bond correlation (HMBC) spectroscopy) were acquired with standard pulse sequences using a Bruker Avance 600 MHz equipped with a triple resonance cryoprobe. 1D ^{13}C and ^{19}F spectra were recorded using a Bruker Avance 400 MHz. All the spectra were processed with Topspin 2.1 (Bruker). The DQF-COSY spectra were collected using data sets of 2048 × 300 points with 16 transients per t1 increment. The data matrix was zero-filled in both dimensions to give a matrix of 4096 × 2048 points and was resolution-enhanced in both dimensions using a cosine bell function before Fourier transformation. The ^{1}H−^{13}C HSQC and ^{1}H−^{13}C HMBC experiments were performed in the ^{1}H detection mode by single-quantum coherence with proton decoupling in the ^{13}C domain using data sets of 2048 × 400 points. The ^{1}H−^{13}C HSQC experiment was performed using sensitivity improvement, and in the phase-sensitive mode using echo/antiecho gradient selection, with multiplicity editing during the selection step,[56] setting the one-bond heteronuclear coupling value to 145 Hz. The ^{1}H−^{13}C HMBC experiment was optimized on long-range coupling constants, with a low-pass J filter to suppress one-bond correlations, using gradient pulses for selection. The data matrix in all the heteronuclear experiments was extended to 2048 × 1024 points using a forward linear prediction.[57]

Identification of additional oxidation products was performed using HRMS analysis and comparison of the experimental UV−vis absorption spectra with standard compounds, or if not available, with literature data. Pure products were collected by RP-HPLC analysis of the reaction mixture and then subjected to MS analysis using an electrospray ionization-time of flight (ESI-TOF) instrument. An isocratic flow of 90% acetonitrile in water with 0.1% formic acid was used as the eluent in all runs. MS analyses were performed in the positive ion mode, exploring a range of m/z values from 100 to 750 Th. 2-Hydroxy-3-oxindole, 2-methoxy-3-oxindole, and 2-ethoxy-3-oxindole were identified based on their EI-MS spectra, collected upon GC−MS analysis as described above.

ASSOCIATED CONTENT

Ⓢ Supporting Information

The Supporting Information is available free of charge at https://pubs.acs.org/doi/10.1021/acscatal.1c01985.

> HPLC chromatograms; UV−vis, ESI-MS, EI-MS, CD, and NMR spectra; identified products obtained upon indole oxidation by Mn-MC6*a under the explored reaction conditions; and far-UV region CD parameters for Mn-MC6*a in aqueous solution at pH 8.5 with different cosolvents (PDF)
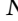
AUTHOR INFORMATION

Corresponding Authors

Flavia Nastri − *Department of Chemical Sciences, University of Napoli Federico II, Napoli 80126, Italy*; Email: flavia.nastri@unina.it

Angela Lombardi − *Department of Chemical Sciences, University of Napoli Federico II, Napoli 80126, Italy*; ⓞ orcid.org/0000-0002-2013-3009; Email: alombard@unina.it

Authors

Linda Leone − *Department of Chemical Sciences, University of Napoli Federico II, Napoli 80126, Italy*; ⓞ orcid.org/0000-0001-7293-1814

Daniele D'Alonzo − *Department of Chemical Sciences, University of Napoli Federico II, Napoli 80126, Italy*; ⓞ orcid.org/0000-0002-2857-8600

Ornella Maglio − *Department of Chemical Sciences, University of Napoli Federico II, Napoli 80126, Italy; Institute of Biostructures and Bioimages—National Research Council, Napoli 80134, Italy*

Vincenzo Pavone − *Department of Chemical Sciences, University of Napoli Federico II, Napoli 80126, Italy*

Complete contact information is available at:
https://pubs.acs.org/10.1021/acscatal.1c01985

Author Contributions

L.L. performed the experiments, analyzed the data, and prepared the manuscript draft. D.D. and L.L. interpreted the data and conceived the mechanistic proposal. O.M. acquired and analyzed the NMR data with support of L.L. V.P., F.N., and A.L. contributed to the design of the experiments and provided critical feedback to the results. F.N. and A.L. edited and finalized the manuscript. A.L. directed the project. All authors participated in the discussion, revised, and approved the manuscript.

Notes

The authors declare no competing financial interest.

ACKNOWLEDGMENTS

REFERENCES

(1) Du, Z.; Shao, Z. Combining Transition Metal Catalysis and Organocatalysis − an Update. *Chem. Soc. Rev.* **2013**, *42*, 1337−1378.

(2) Cohen, S. M. New Approaches for Medicinal Applications of Bioinorganic Chemistry. *Curr. Opin. Chem. Biol.* **2007**, *11*, 115−120.

(3) Yan, Y.; Zhang, J.; Ren, L.; Tang, C. Metal-Containing and Related Polymers for Biomedical Applications. *Chem. Soc. Rev.* **2016**, *45*, 5232−5263.

(4) Lin, Y.-W. Biodegradation of Aromatic Pollutants by Metalloenzymes: A Structural-Functional-Environmental Perspective. *Coord. Chem. Rev.* **2021**, *434*, No. 213774.

(5) Dogutan, D. K.; Nocera, D. G. Artificial Photosynthesis at Efficiencies Greatly Exceeding That of Natural Photosynthesis. *Acc. Chem. Res.* **2019**, *52*, 3143−3148.

(6) Le, J. M.; Bren, K. L. Engineered Enzymes and Bioinspired Catalysts for Energy Conversion. *ACS Energy Lett.* **2019**, *4*, 2168−2180.

(7) Gilardi, G.; Fantuzzi, A. Manipulating Redox Systems: Application to Nanotechnology. *Trends Biotechnol.* **2001**, *19*, 468–476.

(8) Trouvé, J.; Gramage-Doria, R. Beyond Hydrogen Bonding: Recent Trends of Outer Sphere Interactions in Transition Metal Catalysis. *Chem. Soc. Rev.* **2021**, *50*, 3565–3584.

(9) Amanullah, S.; Saha, P.; Nayek, A.; Ahmed, M. E.; Dey, A. Biochemical and Artificial Pathways for the Reduction of Carbon Dioxide, Nitrite and the Competing Proton Reduction: Effect of 2nd Sphere Interactions in Catalysis. *Chem. Soc. Rev.* **2021**, *50*, 3755–3823.

(10) Nastri, F.; D'Alonzo, D.; Leone, L.; Zambrano, G.; Pavone, V.; Lombardi, A. Engineering Metalloprotein Functions in Designed and Native Scaffolds. *Trends Biochem. Sci.* **2019**, *44*, 1022–1040.

(11) Arnold, F. H. Directed Evolution: Bringing New Chemistry to Life. *Angew. Chem., Int. Ed.* **2018**, *57*, 4143–4148.

(12) Chordia, S.; Narasimhan, S.; Lucini Paioni, A.; Baldus, M.; Roelfes, G. In Vivo Assembly of Artificial Metalloenzymes and Application in Whole-Cell Biocatalysis. *Angew. Chem., Int. Ed.* **2021**, *60*, 5913–5920.

(13) Kato, S.; Onoda, A.; Grimm, A. R.; Schwaneberg, U.; Hayashi, T. Construction of a Whole-Cell Biohybrid Catalyst Using a Cp*Rh(III)-Dithiophosphate Complex as a Precursor of a Metal Cofactor. *J. Inorg. Biochem.* **2021**, *216*, No. 111352.

(14) Basler, S.; Studer, S.; Zou, Y.; Mori, T.; Ota, Y.; Camus, A.; Bunzel, H. A.; Helgeson, R. C.; Houk, K. N.; Jiménez-Osés, G.; Hilvert, D. Efficient Lewis Acid Catalysis of an Abiological Reaction in a de Novo Protein Scaffold. *Nat. Chem.* **2021**, *13*, 231–235.

(15) Stenner, R.; Steventon, J. W.; Seddon, A.; Anderson, J. L. R. A de Novo Peroxidase Is Also a Promiscuous yet Stereoselective Carbene Transferase. *Proc. Natl. Acad. Sci.* **2020**, *117*, 1419–1428.

(16) Sigmund, M.-C.; Poelarends, G. J. Current State and Future Perspectives of Engineered and Artificial Peroxygenases for the Oxyfunctionalization of Organic Molecules. *Nat. Catal.* **2020**, *3*, 690–702.

(17) Leone, L.; Chino, M.; Nastri, F.; Maglio, O.; Pavone, V.; Lombardi, A. Mimochrome, a Metalloporphyrin-Based Catalytic Swiss Knife. *Biotechnol. Appl. Biochem.* **2020**, *67*, 495–515.

(18) Di Costanzo, L.; Geremia, S.; Randaccio, L.; Nastri, F.; Maglio, O.; Lombardi, A.; Pavone, V. Miniaturized Heme Proteins: Crystal Structure of Co(III)-Mimochrome IV. *J. Biol. Inorg. Chem.* **2004**, *9*, 1017–1027.

(19) Nastri, F.; Lista, L.; Ringhieri, P.; Vitale, R.; Faiella, M.; Andreozzi, C.; Travascio, P.; Maglio, O.; Lombardi, A.; Pavone, V. A Heme–Peptide Metalloenzyme Mimetic with Natural Peroxidase-Like Activity. *Chem. − Eur. J.* **2011**, *17*, 4444–4453.

(20) Vitale, R.; Lista, L.; Cerrone, C.; Caserta, G.; Chino, M.; Maglio, O.; Nastri, F.; Pavone, V.; Lombardi, A. An artificial heme-enzyme with enhanced catalytic activity: evolution, functional screening and structural characterization. *Org. Biomol. Chem.* **2015**, *13*, 4859–4868.

(21) Caserta, G.; Chino, M.; Firpo, V.; Zambrano, G.; Leone, L.; D'Alonzo, D.; Nastri, F.; Maglio, O.; Pavone, V.; Lombardi, A. Enhancement of Peroxidase Activity in Artificial Mimochrome VI Catalysts through Rational Design. *ChemBioChem* **2018**, *19*, 1823–1826.

(22) Leone, L.; D'Alonzo, D.; Balland, V.; Zambrano, G.; Chino, M.; Nastri, F.; Maglio, O.; Pavone, V.; Lombardi, A. Mn-Mimochrome VI*a: An Artificial Metalloenzyme With Peroxygenase Activity. *Front. Chem.* **2018**, *6*, 590.

(23) Firpo, V.; Le, J. M.; Pavone, V.; Lombardi, A.; Bren, K. L. Hydrogen Evolution from Water Catalyzed by Cobalt-Mimochrome VI*a, a Synthetic Mini-Protein. *Chem. Sci.* **2018**, *9*, 8582–8589.

(24) Kim, W.-H.; Jeong, P.; Kim, S.-Y.; Cho, H.; Lee, J.-M.; Seo, S.; Shen, H.; Ahn, Y.; Jung, D.-W.; Kim, Y.-C.; Williams, D. R. A Novel Indirubin Derivative That Increases Somatic Cell Plasticity and Inhibits Tumorigenicity. *Bioorg. Med. Chem.* **2019**, *27*, 2923–2934.

(25) Kaur, M.; Singh, M.; Chadha, N.; Silakari, O. Oxindole: A Chemical Prism Carrying Plethora of Therapeutic Benefits. *Eur. J. Med. Chem.* **2016**, *123*, 858–894.

(26) Yu, B.; Yu, D.-Q.; Liu, H.-M. Spirooxindoles: Promising Scaffolds for Anticancer Agents. *Eur. J. Med. Chem.* **2015**, *97*, 673–698.

(27) Khan, M.; Yousaf, M.; Wadood, A.; Junaid, M.; Ashraf, M.; Alam, U.; Ali, M.; Arshad, M.; Hussain, Z.; Khan, K. M. Discovery of Novel Oxindole Derivatives as Potent α-Glucosidase Inhibitors. *Bioorg. Med. Chem.* **2014**, *22*, 3441–3448.

(28) Najahi, E.; Valentin, A.; Fabre, P. L.; Reybier, K.; Nepveu, F. 2-Aryl-3H-Indol-3-Ones: Synthesis, Electrochemical Behaviour and Antiplasmodial Activities. *Eur. J. Med. Chem.* **2014**, *78*, 269–274.

(29) Atienza, B. J. P.; Jensen, L. D.; Noton, S. L.; Ansalem, A. K. V.; Hobman, T.; Fearns, R.; Marchant, D. J.; West, F. G. Dual Catalytic Synthesis of Antiviral Compounds Based on Metallocarbene–Azide Cascade Chemistry. *J. Org. Chem.* **2018**, *83*, 6829–6842.

(30) Russell, G. A.; Kaupp, G. Reactions of Resonance Stabilized Carbanions. XXXI. Oxidation of Carbanions. 4. Oxidation of Indoxyl to Indigo in Basic Solution. *J. Am. Chem. Soc.* **1969**, *91*, 3851–3859.

(31) Zhang, X.; Li, P.; Lyu, C.; Yong, W.; Li, J.; Pan, X.; Zhu, X.; Rao, W. Palladium-Catalyzed One-Pot Synthesis of C2-Quaternary Indolin-3-ones via 1H-Indole-3-sulfonates Generated in Situ from 2-Alkynyl Arylazides and Sulfonic Acids. *Adv. Synth. Catal.* **2017**, *359*, 4147–4152.

(32) Lauwick, H.; Sun, Y.; Akdas-Kilig, H.; Dérien, S.; Achard, M. Access to 3-Oxindoles from Allylic Alcohols and Indoles. *Chem. − Eur. J.* **2018**, *24*, 7964–7969.

(33) Devi, L.; Shukla, R.; Rastogi, N. Intramolecular Trapping of Ammonium Ylides with N-Benzoylbenzotriazoles in Aqueous Medium: Direct Access to the Pseudoindoxyl Scaffold. *Org. Biomol. Chem.* **2019**, *17*, 135–139.

(34) Sun, Y.; Fan, R. Construction of 3-Oxyindoles via Hypervalent Iodine Mediated Tandem Cyclization–Acetoxylation of o-Acyl Anilines. *Chem. Commun.* **2010**, *46*, 6834–6836.

(35) Xu, J.; Shoji, O.; Fujishiro, T.; Ohki, T.; Ueno, T.; Watanabe, Y. Construction of Biocatalysts Using the Myoglobin Scaffold for the Synthesis of Indigo from Indole. *Catal. Sci. Technol.* **2012**, *2*, 739–744.

(36) Corbett, M. D.; Chipko, B. R. Peroxide Oxidation of Indole to Oxindole by Chloroperoxidase Catalysis. *Biochem. J.* **1979**, *183*, 269–276.

(37) Zhang, R.; He, Q.; Chatfield, D.; Wang, X. Paramagnetic Nuclear Magnetic Resonance Relaxation and Molecular Mechanics Studies of the Chloroperoxidase–Indole Complex: Insights into the Mechanism of Chloroperoxidase-Catalyzed Regioselective Oxidation of Indole. *Biochemistry* **2013**, *52*, 3688–3701.

(38) Gillam, E. M. J.; Notley, L. M.; Cai, H.; de Voss, J. J.; Guengerich, F. P. Oxidation of Indole by Cytochrome P450 Enzymes. *Biochemistry* **2000**, *39*, 13817–13824.

(39) Barrios, D. A.; D'Antonio, J.; McCombs, N. L.; Zhao, J.; Franzen, S.; Schmidt, A. C.; Sombers, L. A.; Ghiladi, R. A. Peroxygenase and Oxidase Activities of Dehaloperoxidase-Hemoglobin from Amphitrite Ornata. *J. Am. Chem. Soc.* **2014**, *136*, 7914–7925.

(40) Kuo, H. H.; Mauk, A. G. Indole Peroxygenase Activity of Indoleamine 2,3-Dioxygenase. *Proc. Natl. Acad. Sci.* **2012**, *109*, 13966–13971.

(41) Liu, C.; Xu, J.; Gao, S.-Q.; He, B.; Wei, C.-W.; Wang, X.-J.; Wang, Z.; Lin, Y.-W. Green and Efficient Biosynthesis of Indigo from Indole by Engineered Myoglobins. *RSC Adv.* **2018**, *8*, 33325–33330.

(42) Linhares, M.; Rebelo, S. L. H.; Simões, M. M. Q.; Silva, A. M. S.; Neves, M. G. P. M. S.; Cavaleiro, J. A. S.; Freire, C. Biomimetic Oxidation of Indole by Mn(III)Porphyrins. *Appl. Catal. A Gen.* **2014**, *470*, 427–433.

(43) Rebelo, S. L. H.; Linhares, M.; Simões, M. M. Q.; Silva, A. M. S.; Neves, M. G. P. M. S.; Cavaleiro, J. A. S.; Freire, C. Indigo Dye Production by Enzymatic Mimicking Based on an Iron(III)Porphyrin. *J. Catal.* **2014**, *315*, 33–40.

(44) Sacramento, J. J. D.; Goldberg, D. P. Oxidation of an Indole Substrate by Porphyrin Iron(III) Superoxide: Relevance to Indoleamine and Tryptophan 2,3-Dioxygenases. *Chem. Commun.* **2020**, *56*, 3089−3092.

(45) Kang, H.; Jemison, A. L.; Nigro, E.; Kozlowski, M. C. Oxidative Coupling of 3-Oxindoles with Indoles and Arenes. *ChemSusChem* **2019**, *12*, 3144−3151.

(46) Kagawa, T.; Shigehiro, D.; Kawada, K. Trifluoroethoxy Group as a Leaving Group for Regioselective Sequential Substitution Reactions of 5-Trifluoromethylpyrimidine Derivative with Heteroatom Nucleophiles. *J. Fluorine Chem.* **2015**, *179*, 150−158.

(47) Fisher, E. L.; am Ende, C. W.; Humphrey, J. M. 2,2,2-Trifluoroethoxy Aromatic Heterocycles: Hydrolytically Stable Alternatives to Heteroaryl Chlorides. *J. Org. Chem.* **2019**, *84*, 4904−4909.

(48) Rogers, J. L.; MacMillan, J. B. A Labeled Substrate Approach to Discovery of Biocatalytic Reactions: A Proof of Concept Transformation with N-Methylindole. *J. Am. Chem. Soc.* **2012**, *134*, 12378−12381.

(49) Huang, X.; Groves, J. T. Oxygen Activation and Radical Transformations in Heme Proteins and Metalloporphyrins. *Chem. Rev.* **2018**, *118*, 2491−2553.

(50) Arasasingham, R. D.; He, G. X.; Bruice, T. C. Mechanism of Manganese Porphyrin-Catalyzed Oxidation of Alkenes. Role of Manganese(IV)-Oxo Species. *J. Am. Chem. Soc.* **1993**, *115*, 7985−7991.

(51) Lane, B. S.; Burgess, K. Metal-Catalyzed Epoxidations of Alkenes with Hydrogen Peroxide. *Chem. Rev.* **2003**, *103*, 2457−2474.

(52) Ronsein, G. E.; de Oliveira, M. C. B.; de Medeiros, M. H. G.; Di Mascio, P. Characterization of O_2 $(^1\Delta_g)$-Derived Oxidation Products of Tryptophan: A Combination of Tandem Mass Spectrometry Analyses and Isotopic Labeling Studies. *J. Am. Soc. Mass Spectrom.* **2009**, *20*, 188−197.

(53) Merle, P.-L.; Sabourault, C.; Richier, S.; Allemand, D.; Furla, P. Catalase Characterization and Implication in Bleaching of a Symbiotic Sea Anemone. *Free Radical Biol. Med.* **2007**, *42*, 236−246.

(54) Cosnier, S.; Gondran, C.; Wessel, R.; Montforts, F.-P.; Wedel, M. Poly(Pyrrole−Metallodeuteroporphyrin)Electrodes: Towards Electrochemical Biomimetic Devices. *J. Electroanal. Chem.* **2000**, *488*, 83−91.

(55) Giovannetti, R.; Alibabaei, L.; Pucciarelli, F. Spectral and Kinetic Investigation on Oxidation and Reduction of Water Soluble Porphyrin−Manganese(III) Complex. *Inorganica Chim. Acta* **2010**, *363*, 1561−1567.

(56) States, D. J.; Haberkorn, R. A.; Ruben, D. J. A Two-Dimensional Nuclear Overhauser Experiment with Pure Absorption Phase in Four Quadrants. *J. Magn. Reson. (1969)* **1982**, *48*, 286−292.

(57) Stern, A. S.; Li, K.-B.; Hoch, J. C. Modern Spectrum Analysis in Multidimensional NMR Spectroscopy: Comparison of Linear-Prediction Extrapolation and Maximum-Entropy Reconstruction. *J. Am. Chem. Soc.* **2002**, *124*, 1982−1993.